J Solid State Electrochem (2011) 15:1179–1184
DOI 10.1007/s10008-010-1183-9

ORIGINAL PAPER

Exfoliated graphite nanosheets/carbon nanotubes hybrid materials for superior performance supercapacitors

Haibo Wang · Zhihong Liu · Xiao Chen · Pengxian Han · Shanmu Dong · Guanglei Cui

Received: 8 June 2010 / Revised: 20 August 2010 / Accepted: 25 August 2010 / Published online: 14 September 2010

Abstract Nanostructured hybrid material of exfoliated graphite nanosheets and carbon nanotubes (GNSNT) served as supercapacitor electrode materials was presented. The nanostructured hybrid was prepared by a facile chemical reduction method. The hybrid material was characterized by X-ray diffraction technique, transmission electron microscopy, scanning electron microscopy, cyclic voltammetry, galvanostatic charge/discharge cycling, and four-point probe conductivity measurement to represent a well-defined nanostructure possessing a vast number of active sites and delivering the ingredients for a fast effective charge separation network. Our results clearly demonstrated that the hybrid possess a superior performance. A specific capacitance value 266 F/g was obtained for GNSNT hybrid electrode at a current density of 0.1 A/g, while it was only 185 F/g for exfoliated graphite nanosheets (GNS). At a higher current density of 2 A/g, the GNSNT electrode still keeps a specific capacitance of 220 F/g, which is more than double that of GNS. This synergistic effect of the nanostructured hybrid material offers an effective network for charge separation and therefore renders a significantly enhanced specific capacitance and rate capability.

Keywords Exfoliated-graphite nanosheets · Carbon nanotubes · Hybrid · Conducting networks · Supercapacitors

Haibo Wang and Zhihong Liu contributed equally to this work.

Electronic supplementary material The online version of this article (doi:10.1007/s10008-010-1183-9) contains supplementary material, which is available to authorized users.

H. Wang · Z. Liu · X. Chen · P. Han · S. Dong · G. Cui (✉)
Qingdao Institute of Bioenergy and Bioprocess Technology,
Chinese Academy of Sciences,
Qingdao 266101, People's Republic of China
e-mail: cuigl@qibebt.ac.cn

Introduction

Supercapacitors (also referred to as electrochemical capacitors or ultracapacitors) act as a power bridge between batteries and conventional capacitors owing to its moderate energy density with high-power density [1, 2]. The need for supercapacitors has expanded rapidly in recent years.

Carbon-based capacitors have attracted great attention because these materials possess a large family of diversified morphologies with high stability and conductivity [3–13]. 1D carbon materials, carbon nanotubes (CNTs), with excellent electrical conductivity and high surface areas, have been explored for supercapacitors since 1997 with high-rate performance [5–8]. However, high cost limits their application in supercapacitors. Exfoliated graphite nanosheets (GNS), such as graphene [14–16], are emerging as a novel nanostructured carbon material with a potential for electrochemical energy storage device applications due to its unique characteristics of chemical stability, high-electrical conductivity and large surface area. Its surface area does not depend on the distribution pores as activated carbon, but the random stacking of GNS will also form some porous structures, which can also facilitate charge storage. Recently, GNS was demonstrated to promise advantages for supercapacitor application owing to their intrinsic characteristics [17–20]. Techniques for scaling up GNS from natural graphite have been developed, indicating that a large amount of GNS can be facilely prepared [21]. This makes GNS an attractive candidate for the fabrication of supercapacitor electrode when compared with other carbon materials [17–20, 22].

A concept of establishing an effectively conducting network formed by hybrid 1D CNT and 2D materials was demonstrated to improve the electrochemical properties in the field of solar cells and lithium ion batteries [23, 24], in

which a significant synergistic effect on the performance of hybrid materials was reported [23–26]. The GNS can provide conduction pathway to a great area unit mass than CNT. Thus, a GNS/CNT hybrid composite could be expected to establish a highly effective charge separation network. In this case, the carbon nanotubes act as an excellent 1D electron expressway, nevertheless GNS serve as a large 2D electron-conducting square. The novel synergistic network renders a desirable, effective candidate for charge separation and transportation in the device. The nanostructured hybrid formed by exfoliated graphite nanosheets and single-walled carbon nanotubes was fabricated into the electrode of supercapacitors and superior performance was observed. The graphite nanosheets and carbon nanotubes (GNSNT) electrode exhibits a specific capacitance of 266 F/g at a current density of 0.1 A/g, while the GNS-based electrode delivers only 185 A/g under the same condition. Furthermore, the rate capability of GNSNT is drastically enhanced in comparison with that of GNS.

Experimental section

Preparation of graphite oxide, GNS and GNSNT hybrid materials

Graphite oxide was prepared by a modified Hummers method [27]. In a typical preparation of GNS 3 g portion of graphite oxide in 500 mL deionized water were exfoliated in an ultrasonic bath for 5 h and was chemically reduced by 5.0 mL hydrazine hydrate (50%) at room temperature for 24 h to give the black GNS after filtering, washing, and drying.

The preparation of GNSNT hybrid materials was performed as follows. The carbon nanotubes (OD, 2–6 nm, length, ~20 um, purity >95%, SSA >400 m^2/g, EC >102 S/cm, Ash <wt. 3.5%, provided by Chengdu Organic Chemicals Company Ltd. of CAS) was treated in a concentrated H_2SO_4 and HNO_3 mixture at room temperature for 2 h, followed by ultrasonic treatment to separate individual CNT with hydrophilic surfaces. Then, hydrophilic CNT was mixed with the graphite oxide (1: 9 wt.) in water and ultrasonically treated for another 3 h for a homogeneous mixing. The mixture was then reduced with hydrazine hydrate at room temperature for 24 h, followed by filtering and washing with distilled water, and to provide the GNSNT hybrid materials after drying in a vacuum oven at 70 °C.

Sample characterization

X-ray diffraction pattern (XRD) patterns were recorded in a Bruker-AXS Micro-diffractometer (D8 ADVANCE) with Cu Kα radiation (λ=1.5406) from 5° to 70° at a scanning speed of 0.33°/min. X-ray tube voltage and current were set at 40 kV and 40 mA, respectively. Morphological and structural information were attained from field emission scanning electron microscopy (HITACHI S-4800). For transmission electron microscopy (TEM) study, the sample was dispersed in 2 mL of absolute ethanol, followed by sonicating for 20 min. The samples were picked up by immersing a carbon-coated 200-mesh copper grid into the solution for a few seconds and dried under ambient conditions for imaging. Brunauer-Emmett-Teller (BET) surface area measurement was done using a micromeritics Instrument ASAP2020.

Electrical conductivity measurements

The electrical conductivities of the GNS or GNSNT pellets were measured using the four-probe technique on a four-point probe Resistivity Measurement System (RTS-8, Four Probes Tech.) at room temperature. The pellets were 10.0 mm in diameter and 0.5–0.8 mm in thickness, and were pressed at room temperature pressure of 40 MPa for 5 min. Three pellets were tested and each pellet was measured four times in different position. The average of the 12 conductivity values was adopted as the conductivity of the pellets.

Electrochemical measurements

Two-electrode Swagelok-type system was employed to study the electrochemical performance of the GNS, CNT, and GNSNT electrodes in a 30 wt.% KOH aqueous system, respectively. The electrodes were prepared by mixing the samples (GNS, CNT, or GNSNT) with 10 wt.% PTFE binder and pasted on a stainless steel current collector under a pressure of 15 MPa. A unit cell for the capacitor was fabricated with two electrodes (typically containing 8 mg of active materials) separated by polypropylene separator in 30% KOH aqueous solution as the electrolyte. The electrochemical properties of the electrodes were evaluated by cyclic voltammetry (CV) using a CHI 440A instrument (CHI Instrument Inc.) and galvanostatic charge/discharge measurements conducted with a charge–discharge tester. The cyclic voltammetry response of the electrodes were measured at different sweep rates varying from 10 to 200 mV/s. Galvanostatic charge/discharge was carried out at potentials between a voltage window of 0 and 1.0 V. Impedance spectroscopy measurements were carried out at a dc bias of 0.1 V with sinusoidal signal of 5 mV over the frequency range from 100 kHz to 10 mHz.

Results and discussion

XRD patterns of the parent graphite, graphite oxide, and resultant exfoliated graphite nanosheets are shown in Fig. S1.

A sharp peak at 26.5° can be indexed to (002) diffractions of graphite and calculated d-spacing is 0.335 nm, while a typical (001) peak located at 10.3°, corresponding to an interlayer spacing of 0.776 nm for the graphite oxide. This result indicates that graphite is transformed into graphite oxide and most oxygen-containing groups are chemically bonded to the planar surface of graphite after the oxidization. After reducing, followed by the low-temperature heat-treatment procedure, the sharp peak of around 10.3° at the XRD patterns disappears and a weak band at 24.7° emerges, indicating that oxygen containing groups are largely removed during the chemical reduction.

Some representative SEM and TEM images of GNS and GNSNT are shown in Fig. 1. The typical morphology of agglomerated and rippled GNS was observed. The CNT are homogenously dispersed between the GNS particles and/or embedded in the aggregated GNS, which is consistent with the previous results that these two carbon materials are quite miscible (shown in Fig. 1c) [23–26, 28]. This unique hybrid structure is advantageous for the electrochemical performance of capacitors because the CNT can bridge the GNS particles and form an effective conducting network (shown in Fig. 1e). Moreover, the surface area of the GNS and GNSNT samples as measured by the N_2 absorption BET method is 240.8 and 296.2 m^2/g, respectively. This means that the rigid CNT between the GNS prevent the agglomeration of flexible GNS and enlarge the specific surface area.

A good electrical conductivity is a prerequisite of superior performance of supercapacitor. Before electrochemical measurements, the electrical conductivity of GNSNT and GNS samples was tested by four-point probe technique. As a result, the electrical conductivity of GNSNT in this study is observed to be 1.41 S/cm, fivefold greater than that of GNS (0.24 S/cm).

The two-electrode test cell configuration was applied to evaluate nanostructured hybrid's performance for supercapacitors [29]. CVs tests have been performed on GNS, GNSNT, and CNT capacitors, respectively, between the voltage limits of 0–1.0 V in 30% KOH solution. The CVs of GNSNT and GNS capacitors at sweep rates ranging from 10 to 200 mV/s are displayed in Fig. 2. Almost rectangular shaped CV curves were obtained for both GNSNT and CNT at low scanning rate, which indicates that GNSNT and GNS possess good capacitive properties in 30% KOH electrolytes [19]. With increasing the sweep rate, which accelerates the build-up of the electric double layer, the rectangles for the GNS samples became more inclined (45° to the voltage axis) than those of the GNSNT samples. The slope of V/I (indicated by the dotted box) is reported to be closely related with the equivalent series resistance (ESR). [30] The CV curves of the GNSNT samples display much greater slope than GNS samples, which mean a smaller ESR compared with that of GNS. To examine the effect of the CNT on the electrochemical properties of GNSNT, CVs tests on pure CNT were also conducted (Fig. S2). As can be seen, CV curves of the CNT-based capacitors are close to an ideal rectangular shape at each sweep rate, which presents very excellent rate performance. The CV results of GNS, CNT, and GNSNT indicate that addition of CNT in GNS is beneficial to decrease the resistance and improve the electrochemical performance of GNSNT capacitors [31, 32]. Therefore, it is reasonable that the hybrid form an effectively nanostructured network, which facilitate diffusion of electrolyte and improve mass transport properties because CNT wiring the GNS enhances the conductivity

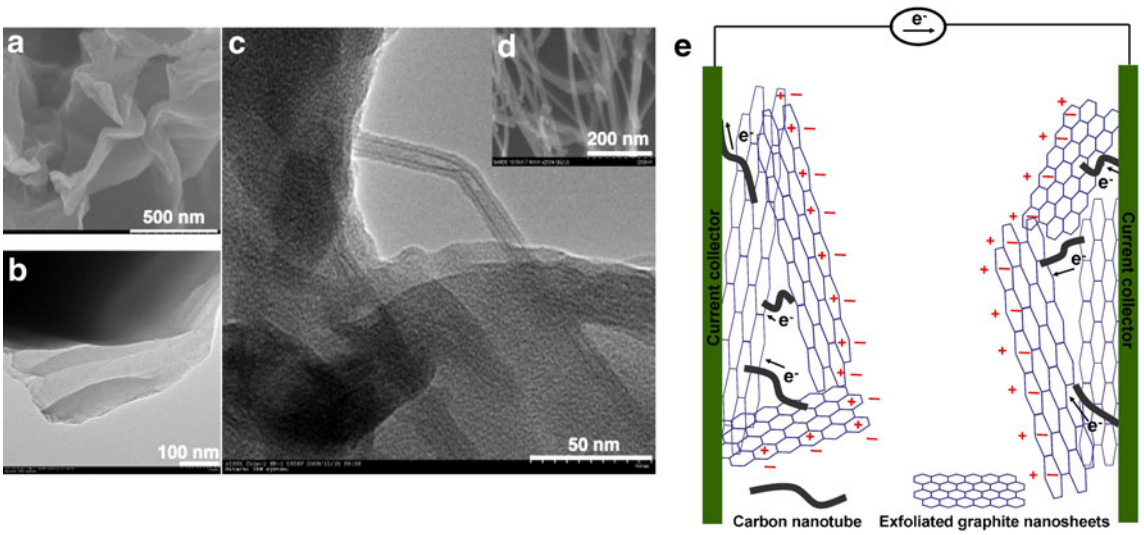

Fig. 1 **a** SEM image of GNS, **b** TEM image showing individual sheets extending from GNS, **c** TEM image of GNSNT hybrid materials and the inset, **d** SEM image of CNT after ultrasonic treatment, **e** corresponding schematic illustration of the electronically conducting network of GNSNT hybrid material

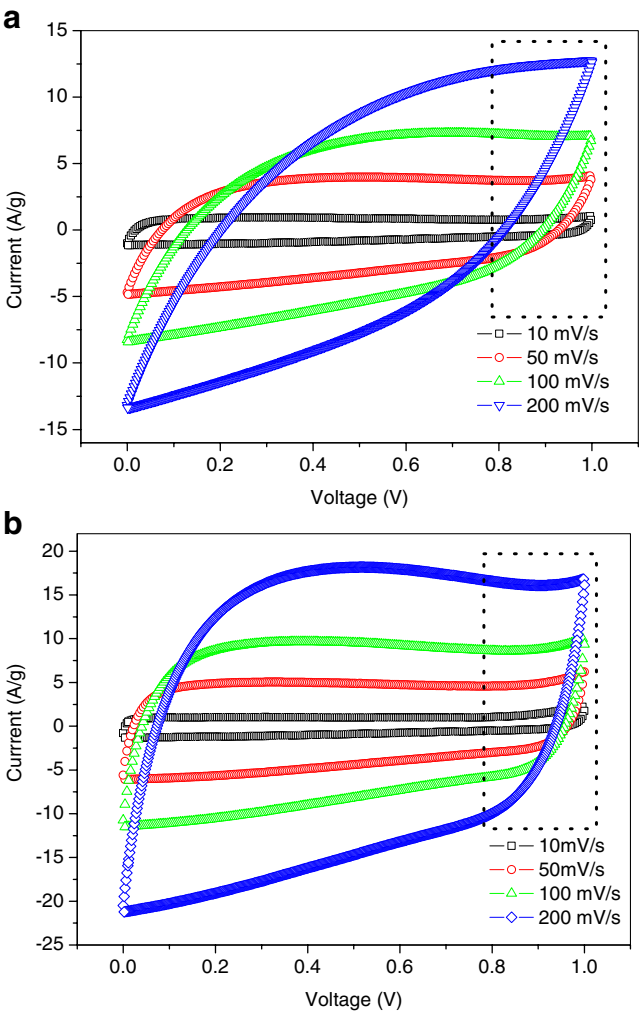

Fig. 2 CV curves of **a** GNS and **b** GNSNT samples at varying sweep rates in 30% KOH aqueous solution

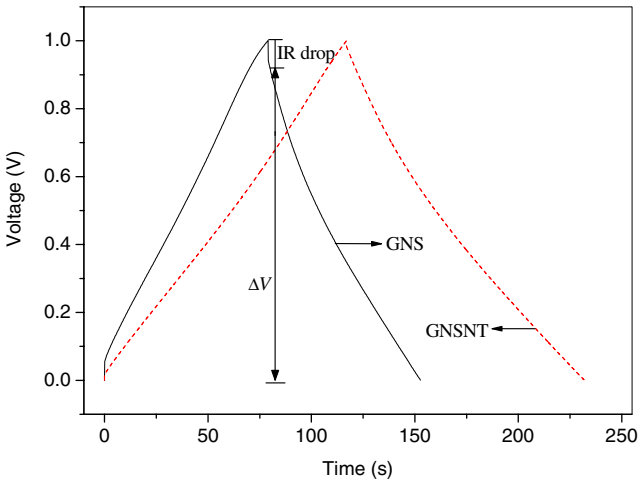

Fig. 3 Galvanostatic charge/discharge curves of GNS and GNSNT electrodes at a current density of 1 A/g

and CNT inserting GNS provide much more accessible surface area [26].

To illustrate how the hybrid nanostructure would influence the performance of capacitance, a galvanostatic charge/discharge experiments were conducted between the voltage windows of 0–1 V to evaluate the performance. The specific capacitance (C) is calculated from the slope of the charge–discharge curves, according to the equation:

$$C = \frac{2 \times I \times \Delta t}{m \Delta V} \quad (1)$$

where, m is the mass of the electrode, and I, Δt, ΔV are the discharging current, time, and voltage, respectively. As shown in Fig. 3, both GNSNT and CNT electrodes show a linear galvanostatic charge/discharge curve at a loading current of 1 A/g. It also can be seen that a sudden potential drop at the very beginning of discharge (IR drop). This phenomenon is usually associated with the ESR of the capacitor at the beginning of discharge [33]. The IR drops from the GNSNT-based electrode are obviously lower than that from the GNS-based one.

The key factors determining the IR drop of supercapacitors are bulk solution resistance, electrode resistance and ion-migration resistance in the electrode [34]. The IR drop was measured and plotted against the discharge current (Fig. 4). It can be shown that the IR drop increase linearly with the current. The slope of the resulting diagram can be used to estimate the overall resistance of the capacitor [35]. Greater slope (K) represents higher overall resistance of the capacitor. From Fig. 4, the slope for GNS samples were nearly double than that for GNSNT samples, which confirms that the conductivity of GNSNT electrode is superior than that of GNS electrode.

Generally speaking, larger currents density may enhance the IR drop and thus reduce of the specific capacitance. Current densities ranging from 0.1 to 2 A/g as a function of specific capacitance of capacitors with GNS and GNSNT are plotted in Fig. 5. For comparison, the specific capacitance of CNT capacitors as a function of charge/discharge current density was also conducted (Fig. S3). From Fig. 5, it can be seen that the discharge capacitances of both capacitors decrease similarly with increasing discharge current density, while the capacitance of capacitor with GNSNT is still generally better than those with GNS at each current density, particularly at higher current densities. For example, the specific capacitance values of 185 and 266 F/g were obtained for the GNS and GNSNT electrodes respectively at a low current density of 0.1 A/g. While at a high current density of 2 A/g, the specific capacitance of the GNSNT electrode is 220 F/g, which is more than double that of GNS (105.6 F/g). It should be noted that the electrical conductivity of the GNSNT samples is fivefold greater that of the GNS sample. In the case of GNSNT-based electrodes, the CNT (has electrical conductivity of

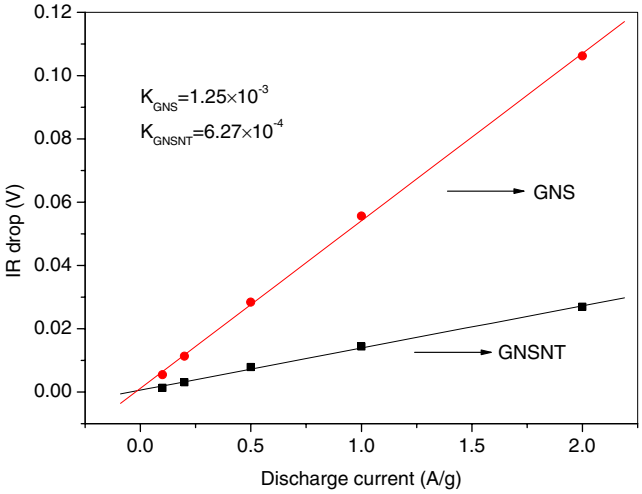

Fig. 4 Variation of IR drop with discharge current for the GNSNT (*black square*) and GNS (*black circle*) samples (*K* is the slope of the curve)

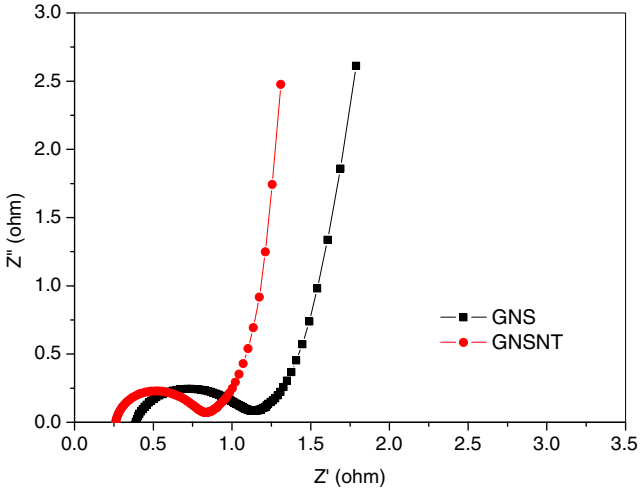

Fig. 6 Nyquist plots for GNS (*black square*) and GNSNT (*black circle*) electrodes at a dc bias of 0.1 V with sinusoidal signal of 5 mV over the frequency range from 100 kHz and 0.1 Hz

about 10^2 S/cm) bridging between the GNS build up an effective conductivity network, which is vital for sufficient utilization of surface of GNS.

The Nyquist plots of supercapacitor with GNS and GNSNT electrodes, respectively, are shown in Fig. 6. As can be seen, both ac impedance spectra consist of a high-frequency semicircle and a low-frequency line. The high frequency loop is related to the electronic resistance between the GNS [19] and the GNS–current collector interface [36]. Smaller semicircles observed for GNSNT electrodes are indicative of lower interfacial charge–transfer resistance, which can be attributed to the high electrical conductivity and unique hybrid structure. A straight 45° sloped line followed the semicircle in the low frequency region is the Warburg resistance resulting from the frequency dependence of ion diffusion/transport in the electrolyte. The vertical shape at lower frequencies indicates a pure capacitive behavior, representative of the ion diffusion in the structure of the electrode [37]. The magnitude of ESR can be obtained from the *x*-intercept of the Nyquist plot directly. It is obvious that GNSNT electrodes give smaller ESR and better capacitive behavior than GNS, which agrees well with previous CV results.

Cycling performance is one of the most important issues concerned for electrochemical capacitors. Cyclic tests of GNS and GNSNT based capacitors were performed at a current density of 0.5 A/g in the range 0–1 V and the results are shown in Fig. 7. It can be seen that the cycling stability of the GNSNT capacitor is a slightly better than GNS capacitors. After 1,000 cycles, the GNSNT electrode shows about 93% of retention of the initial capacitance, whereas the GNS

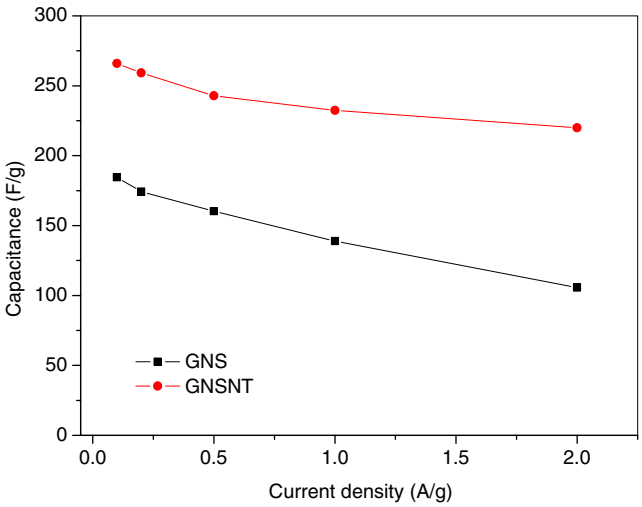

Fig. 5 Specific capacitance of GNS (*black square*) and GNSNT (*black circle*) capacitors as a function of charge/discharge current density in 30% KOH aqueous solution

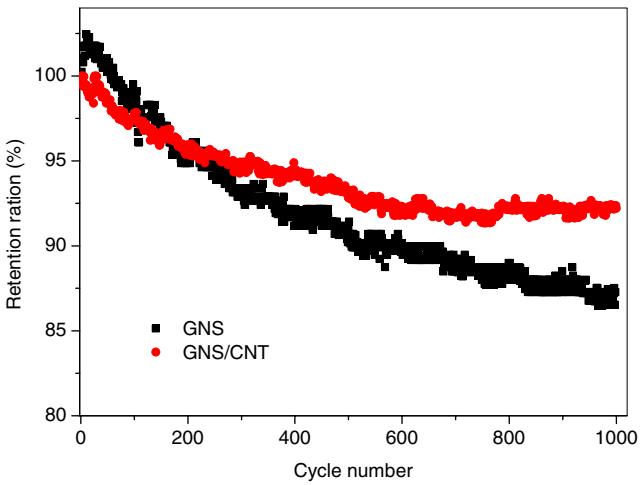

Fig. 7 Cycling performance of GNS (*black square*) and GNSNT (*black circle*) capacitors at a loading current density of 0.5 A/g

exhibits about 86% retention of the initial capacitance. It seemed that the nanostructured network had no significant contribution to the cyclic durability of the carbon-based capacitors. Overall, the nanotructured hybrid materials exhibit better electrochemical behavior than GNS.

Conclusions

Nanostructured hybrid GNSNT was prepared by a facile in situ chemical reduction method with hydrazine hydrate. The GNSNT electrode presents a specific capacitance of 266 F/g at a current density of 0.1 A/g, while for the GNS-based electrode it shows 185 F/g under the same condition. The GNSNT hybrid is observed to still keep a specific capacitance of 220 F/g at a higher current density of 2 A/g, which is nearly double that for GNS electrode. This synergistic effect originates from the unique nanostructured conducting network, which can provide an enhanced electron conduction and charges separation network. These intriguing features make it quite a promising material for application in high-power devices.

Acknowledgments We appreciate the support of "100 Talents" program of the Chinese Academy of Sciences, and National Natural Science Foundation of China (Grant Nos. 20901044, 20971077, and 20902052).

References

1. Fan LZ, Maier J (2006) Electrochem Commun 8:937
2. Zhang LL, Zhao XS (2009) Chem Soc Rev 38:2520
3. Cui GL, Zhi LJ, Müllen K (2007) Chem Phys Chem 8:1013
4. Raymundo PE, Leroux F, Beguin F (2006) Adv Mater 18:1877
5. Niu CM, Sichel EK, Hoch R, Moy D (1997) Appl Phys Lett 70:1480
6. Diederich L, Barborini E, Piseri P, Podesta A, Milani P (1999) Appl Phys Lett 75:2662
7. An KH, Kim WS, Park YS, Moon JM, Bae DJ, Lim SC, Lee YS, Lee YH (2001) Adv Funct Mater 11:387
8. Liu CG, Liu M, Li F, Cheng HM (2008) Appl Phys Lett 92:143108
9. Ania CO, Khomenko V, Raymundo-Pinero E, Parra JB, Beguin F (2007) Adv Funct Mater 17:1828
10. Wang D, Li F, Liu M, Lu GQ, Cheng HM (2008) Angew Chem Int Ed 47:373
11. Feng XL, Liang YY, Zhi LJ, Thomas A, Wu DQ, Lieberwirth I, Kolb U, Müllen K (2009) Adv Funct Mater 19:2125
12. Xu B, Wu F, Chen R, Cao G, Chen S, Zhou Z, Yang YS (2008) Electrochem Commun 10:795
13. Fang B, Binder L (2006) J Power Sources 163:616
14. Novoselov KS, Geim AK, Morozov SV, Jiang D, Zhang Y, Dubonos SV, Grigorieva IV, Firsov AA (2004) Science 306:666
15. Geim AK, Novoselov KS (2007) Nat Mater 6:183
16. Rouhanipour A, Roy M, Feng XL, Räder HJ, Müllen K (2009) Angew Chem Int Ed 48:4602
17. Vivekchand RC, Rout CS, Subrahmanyam KS, Govindaraj A, Rao CNR (2008) J Chem Sci 120:9
18. Meryl D, Stoller PS, Zhu YW, An JH, Ruoff RS (2008) Nano Lett 8:3498
19. Wang Y, Shi ZQ, Huang Y, Ma YF, Wang CY, Chen MM, Chen YS (2009) J Phys Chem C 113:13103
20. Lv W, Tang DM, He YB, You CH, Shi ZQ, Cheng X, Chen CM, Hou PX (2009) ACS Nano 3:3730
21. Li D, Müller M, Gilje S, Kaner RB, Wallace GG (2008) Nat Nanotechnol 3:101
22. Wang DW, Li F, Zhao JP, Ren WC, Chen ZG, Tan J, Wu ZS, Gentle I, Lu GQ, Cheng HM (2009) ACS Nano 3:1745
23. Cai DY, Song M, Xu CX (2008) Adv Mater 20:1706
24. Tung VC, Chen LM, Allen MJ, Wassei JK, Nelson K, Kaner RB, Yang Y (2009) Nano Lett 9(5):1949
25. Yu AP, Ramesh P, Sun XB, Bekyarova E, Itkis ME, Haddon RC (2008) Adv Mater 20:4740
26. Yoo E, Kim J, Hosono E, Zhou HS, Kudo T, Honma I (2008) Nano Lett 8:2277
27. Hummers WS, Offeman RE (1958) J Am Chem Soc 80:1339
28. Liu B, Aydil ES (2009) J Am Chem Soc 131:3985
29. Khomenko V, Frackowiak E, Beguin F (2005) Electrochim Acta 50:2499
30. An KH, Kim SW, Park YS, Moon JM, Bae DJ, Lim SC, Lee YS, Lee YH (2001) Adv Funct Mater 11:391
31. Frackowiak E, Beguin F (2001) Carbon 39:937
32. Zhou HS, Zhu SM, Hibino M, Honma I (2003) J Power Sources 122:219
33. Conway BE (1999) Kluwer Academic, New York
34. Wang KP, Teng HS (2006) Carbon 44:3218
35. Nian YR, Teng HS (2002) J Electrochem Soc 149:A1008
36. Portet C, Taberna PL, Simon P, Laberty-Robert C (2004) Electrochim Acta 49:905
37. Zhang K, Zhang LL, Zhao XS, Wu JS (2010) Chem Mater 22:1392